Carcinogenesis vol.29 no.12 pp.2267–2278, 2008
doi:10.1093/carcin/bgn216
Advance Access publication September 12, 2008

Redox mechanisms switch on hypoxia-dependent epithelial–mesenchymal transition in cancer cells

Stefania Cannito, Erica Novo, Alessandra Compagnone, Lorenzo Valfrè di Bonzo, Chiara Busletta, Elena Zamara, Claudia Paternostro, Davide Povero, Andrea Bandino, Francesca Bozzo, Carlo Cravanzola, Vittoria Bravoco, Sebastiano Colombatto and Maurizio Parola*

Dip. Medicina e Oncologia Sperimentale and Centro Interuniversitario di Fisiopatologia Epatica, University of Torino, Corso Raffaello 30, 10125 Torino, Italy

*To whom correspondence should be addressed. Tel: +39 011 6707772; Fax: +39 011 6707753;
Email: maurizio.parola@unito.it

Epithelial–mesenchymal transition (EMT) and hypoxia are considered as crucial events favouring invasion and metastasis of many cancer cells. In this study, different human neoplastic cell lines of epithelial origin were exposed to hypoxic conditions in order to investigate whether hypoxia *per se* may trigger EMT programme as well as to mechanistically elucidate signal transduction mechanisms involved. The following human cancer cell lines were used: HepG2 (from human hepatoblastoma), PANC-1 (from pancreatic carcinoma), HT-29 (from colon carcinoma) and MCF-7 (from breast carcinoma). Cancer cells were exposed to carefully controlled hypoxic conditions and investigated for EMT changes and signal transduction by using morphological, cell and molecular biology techniques. All cancer cells responded to hypoxia within 72 h by classic EMT changes (fibroblastoid phenotype, SNAIL and β-catenin nuclear translocation and changes in E-cadherin) and by increased migration and invasiveness. This was involving very early inhibition of glycogen synthase kinase-3β (GSK-3β), early SNAIL translocation as well as later and long-lasting activation of Wnt/β-catenin-signalling machinery. Experimental manipulation, including silencing of hypoxia-inducible factor (HIF)-1α and the specific inhibition of mitochondrial generation of reactive oxygen species (ROS), revealed that early EMT-related events induced by hypoxia (GSK-3β inhibition and SNAIL translocation) were dependent on transient intracellular increased generation of ROS whereas late migration and invasiveness were sustained by HIF-1α- and vascular endothelial growth factor (VEGF)-dependent mechanisms. These findings indicate that in cancer cells, early redox mechanisms can switch on hypoxia-dependent EMT programme whereas increased invasiveness is sustained by late and HIF-1α-dependent release of VEGF.

Introduction

Hypoxic conditions have been detected in several human malignancies, including cancers of the breast, prostate, lung, pancreas, rectum, uterine cervix, vulva, head and neck, brain tumours, melanomas, soft tissue sarcomas, non-Hodgkin lymphomas, metastatic liver tumours and renal cell cancer (1,2). Hypoxic or anoxic areas, usually found as heterogeneously distributed areas within solid tumours, may depend either on poor/altered vascularization (perfusion-limited O_2 delivery), deterioration of diffusion geometry (diffusion-limited O_2 delivery) or, to a less extent, to conditions of tumour- or therapy-associated anaemia (1). Although low oxygen tension may even contribute to kill some tumour cells (1,3), hypoxia is more probably to provide a strong selective pressure able to regulate tumour growth and eventually favour survival of the most aggressive malignant cells (4–6). Along these lines, hypoxia within a neoplastic mass is considered as an independent prognostic indicator of poor outcome with a significant risk to develop metastasis that may escape therapy (1,3,7–9). Indeed, neoplastic cells surviving to hypoxia exhibit enhanced invasive propensity, suggesting that hypoxia may favour cancer progression (5,6,10,11). However, the precise mechanisms by which hypoxic conditions may affect progression still remain incompletely understood.

Under hypoxic conditions, cells respond by stabilizing hypoxia-inducible factor (HIF)-1α that, in turn, dimerizes with HIF-1β, translocates into the nuclei and binds to a specific sequence defined hypoxia-responsive element, present in the promoter on several hypoxia-dependent target genes. This activates a complex genetic programme designed to sustain several changes necessary to efficiently counteract the decrease in oxygen tension (12–14). Accordingly, HIF-1α, that is overexpressed in many human cancers (15,16), has been proposed to activate transcription of genes involved in crucial features of cancer biology like angiogenesis, cell survival, glucose metabolism and invasiveness (17,18) and then representing a 'putative' target for a selective cancer therapy.

Recently, several reports provided by different laboratories have suggested that the process of epithelial–mesenchymal transition (EMT) may be crucial for cancer progression (19–26). EMT, originally identified as a crucial differentiation and/or morphogenetic process during embryogenesis, is now recognized as a process able to contribute to the development of tissue fibrosis and metastatic malignancies (19–25). In particular, during progression to metastatic competence, carcinoma cells have been described to enter into an EMT programme allowing them to acquire features of mesenchymal-like cells that may significantly favour invasiveness, including changes in adhesive properties, activation of motility and the ability to degrade/remodel extracellular matrix. EMT and its related consequences such as increased motility and invasiveness have been also characterized in cultured cancer cells, offering a chance to investigate molecular mechanisms involved. Although EMT may represents only part of the process leading to cancer cell invasiveness and metastasis, it is remarkable that signalling pathways described to regulate EMT during embryogenesis are also activated during tumour progression (19–25), including those elicited by (i) growth factors acting through receptor–tyrosine kinases like hepatocyte growth factor, fibroblast growth factor and platelet-derived growth factor; (ii) transforming growth factor β; (iii) Jagged and Delta-like ligands that signal through Notch receptors and CSL transcription factor and (iv) Wnt ligands that signals through the pathway involving β-catenin and LEF-1/TCF transcription factor (19–25), with a major role for glycogen synthase kinase-3β (GSK-3β) as a key regulator of SNAIL (26,27). Even more remarkable, it has been recently proposed that cancer stem cells may represent the critical contributors of EMT process in the context of a growing tumour mass (28).

In the present study, evidence is provided suggesting that moderate hypoxic conditions *per se* can trigger, as an independent factor, an EMT programme leading different human cancer cells to significantly increase invasiveness. Hypoxia-dependent changes occurs through a biphasic mechanism involving (i) a very early and reactive oxygen species (ROS)-dependent inhibition of GSK-3β, followed by early SNAIL nuclear translocation and E-cadherin down-regulation that can switch on EMT programme and (ii) a later sequence of events also involving nuclear translocation of β-catenin, with increased invasiveness being effectively sustained by late and HIF-1α-dependent autocrine–paracrine release of vascular endothelial growth factor (VEGF)-A.

Abbreviations: DPI, diphenyl-phenylene iodonium; EMT, epithelial–mesenchymal transition; Erk, extracellular signal-regulated kinase; GSK-3β, glycogen synthase kinase-3β; HIF, hypoxia-inducible factor; PI3-K, phosphatidylinositol 3-kinase; ROS, reactive oxygen species; Rot, Rotenone; siRNA, short interfering RNA; uPAR, urokinase-type plasminogen activator; VEGF, vascular endothelial growth factor.

Materials and methods

Materials

Enhanced chemiluminescence reagents, nitrocellulose membranes (Hybond-C extra) and secondary Cy3-conjugated antibodies were from Amersham Pharmacia Biotech (Cologno Monzese, Milan, Italy). Human recombinant VEGF was from PeproTech (Rocky Hill, NJ). Monoclonal antibodies raised against E-cadherin, N-cadherin, fibronectin, β-catenin as well as antibodies against phosphorylated or total extracellular signal-regulated kinase (Erk)1/2 and c-Akt were from Santa Cruz Biotechnology (Santa Cruz, CA). Antibody against phosphorylated or total GSK-3β were from Cell Signaling Technology (Beverly, MA). Monoclonal antibodies for α-smooth muscle actin and β-actin were from Sigma Aldrich Spa (Milan, Italy). The polyclonal antibody against SNAIL was from AbCAM (Cambridge, UK). The monoclonal neutralizing antibody against VEGF receptor type 2 (Flk-1) was obtained from ImClone (New York, NY). Matrigel was provided by BD Biosciences Italia (Buccinasco, Italy). All other reagents, including pegylated superoxide dismutase and pegylated catalase, were of analytical grade and obtained from Sigma Chemical Co (Sigma Aldrich Spa).

Cell lines and culture conditions

All human cancer cell lines (HepG2, originally derived from a human hepatoblastoma; PANC-1 from human pancreatic carcinoma; HT-29 from human colon adenocarcinoma and MCF-7 from human breast carcinoma) were obtained from American Type Culture Collection (Manassas, VA). HepG2, Panc-1 and MCF-7 cells were maintained in Dulbecco's modified Eagle's medium, whereas HT-29 cells were maintained in McCoy's medium. All culture media were supplemented with 10% fetal bovin serum, 100 U/ml penicillin, 100 μg/ml streptomycin and 25 μg/ml amphotericin B. Cells were amplified at 37°C in a humidified incubator with 5% CO_2 and 95% air. In experiments designed to evaluate the role of hypoxia, cells were first seeded in normoxic conditions to obtain the desired subconfluence level (65–70%) and then were incubated in strictly controlled hypoxic conditions (3% O_2), as previously detailed elsewhere (29,30) for up to 72 h. Human recombinant Wnt3A employed in this study was purified from culture medium of engineered L-Wnt-3A cells (American Type Culture Collection) as described by others (31).

Western blot analysis

Total cell lysates, nuclear and cytosolic extracts were obtained as previously detailed (29,30,32,33). Lysates or extracts were then subjected to sodium dodecyl sulphate–polyacrylamide gel electrophoresis on 12, 10 or 7.5% acrylamide gels. The blots were incubated with desired primary antibodies and then incubated with peroxidase-conjugated anti-mouse or anti-rabbit immunoglobulins in Tris-buffered saline–Tween containing 2% (wt/vol) non-fat dry milk, as described previously (30,32–35) and developed with the enhanced chemiluminescence reagents according to the manufacturer's instructions. When necessary, immunoprecipitation was performed on cell lysates or culture medium by using Protein A-Sepharose beads, as described in detail elsewhere (32,33).

Cell migration and invasion assays

Cell migration and invasion assays were performed and evaluated as recently described in details (36) by employing Boyden chambers equipped with 8 μm porosity polyvinylpyrrolidone-free polycarbonate filters that were coated either with 20 μg/mg human collagen type I (Collaborative Biomedical Products, Bedford, MA) for cell migration assay or with 50 μg/ml of Matrigel solution for invasion assay. Cell migration and invasiveness were quantified by counting, with a Zeiss microscope (Oberkochen, Germany) equipped with bright-field optics (×40), crystal violet-stained cells that either migrated to the lower surface of collagen-coated polycarbonate filters or invaded Matrigel, respectively. For each filter/Matrigel, the number of cells in 10 randomly chosen fields was counted, and the counts were averaged (means ± SD). Results are expressed as the number of migrated cells per high-power field.

Indirect immunofluorescence

Indirect immunofluorescence was performed on cells seeded on six-well culture plates as described previously (29,34). Briefly, cells were fixed with methanol:acetone 1:1 (vol/vol) for 20 min at −20°C and then permeabilized with phosphate-buffered saline containing 0.5% Triton X-100 and 0.05% NaN_3 (sodium azide) for 10 min at room temperature. Cells were then incubated with primary antibodies overnight at 4°C. Immunopositivity was revealed by means of appropriate Cy3-conjugated antibodies (1:1000 dilution). Nuclear staining (blue fluorescence) was obtained by treating cells with 4,6-diamidino-2-phenylindole (1 mg/ml in methanol) for 30 min at room temperature (29,30,34).

Detection of intracellular generation of ROS

HepG2 cells were seeded in 12-well culture plates (10^5 cells per well). Cells were then either exposed to hypoxia for 15 min or, for comparative purposes, treated or not with 50 μM H_2O_2 under normoxic conditions. Intracellular generation of ROS has been detected by using the conversion of 2′,7′-dichlorodihydrofluorescein diacetate (used at 5 μM concentration), once taken up by cells and deacetylated by esterase, into the corresponding fluorescent derivative (37). Cells were observed and photographed under a Zeiss fluorescence microscope.

Analysis of cell death

In preliminary experiments, designed to evaluate induction of cell death in neoplastic cells exposed to hypoxic conditions up to 72 h, necrotic as well as apoptotic cell death were evaluated by analysing lactate dehydrogenase release in culture medium, 4,6-diamidino-2-phenylindole fluorescence staining and fluorometric caspase-3-like activity, as described previously (35,38,39).

HIF-1α silencing by small RNA interference

RNA interference experiments to knockdown HIF-1α expression in HepG2 and HT-29 cells were performed using short interfering RNA duplex (Qiagen Italia, Milano, Italy). The following target sequence was used: 5′-AGGAAGAACTATGAACATAAA-3′. The siRNA and related non-silencing control (negative control) were transfected in HepG2 and HT-29 cells with lipofectamine transfection reagent (Invitrogen srl, Milano, Italy) according to the manufacturer's instructions up to 72 h. Transfected cells in fresh medium were then exposed for further 48 h to the desired experimental conditions and then harvested for sample preparation.

Statistical analysis

Data in bar graphs represent means ± SEM and were obtained from average data of at least three independent experiments. Luminograms and morphological images are representative of at least three experiments with similar results. Statistical analysis was performed by Student's *t*-test or analysis of variance when appropriate ($P < 0.05$ was considered significant).

Results

Hypoxic conditions induce EMT and increased invasiveness in human cancer cells

In preliminary experiments, 65–70% subconfluent cancer cells from all cell lines were exposed to hypoxic conditions (3% O_2) up to 72 h. As expected, this resulted in a significant recruitment and nuclear translocation of HIF-1α but no significant change in cell number or viability, in term of LDH release or of apoptotic indexes like positive 4,6-diamidino-2-phenylindole staining or caspase-3-like activity, was detected (data not shown). All human cancer cells exposed to hypoxia up to 72 h underwent typical EMT morphological and cellular changes (19–26): cancer cells started to loose cell contacts, scattered from cell clusters and acquired a spindle-shaped and fibroblast-like phenotype (Figure 2A). Cancer cells with the time exhibited down-regulation of E-cadherin expression, as detected either by immunofluorescence (Figure 1A and B) or, for HepG2 cells (chosen as a reference cell line here and in most of the experiments designed to investigate molecular mechanisms in detail) also by monitoring E-cadherin protein levels by western blotting (Figure 1B). Transition into mesenchymal-like phenotype of hypoxic HepG2 cells was also accompanied by up-regulation of N-cadherin, α-smooth muscle actin and fibronectin (Figure 1B). Although the degree of up-regulation of mesenchymal markers was found to vary within the different neoplastic cell lines (see comparative data resumed in supplementary Figure 1A, available at *Carcinogenesis* Online), the simple exposure to hypoxia led all cancer cells to show a progressive change into a fibroblastoid-like morphology, to decrease their E-cadherin expression and, of relevance, to significantly increase their ability to migrate and invade Matrigel (see data in Figure 1A and B, Figure 2A–C).

In order to establish whether increased invasiveness was dependent on autocrine–paracrine factors released by cancer cells under hypoxia, conditioned culture media (HYP medium) were collected at 48 h and then used in invasion assay performed in normoxic conditions. HYP medium induced a significant increase in invasiveness in all cancer cells (Figure 2B) that was significantly inhibited when cells, designed to be incubated either under hypoxic conditions or exposed to HYP medium under normoxia, were pre-treated with anti-Flk1 neutralizing antibody (Figure 2B), suggesting a role for VEGF in mediating invasion. Conceptually, identical results were obtained when HepG2 cells were used in homologous experimental conditions

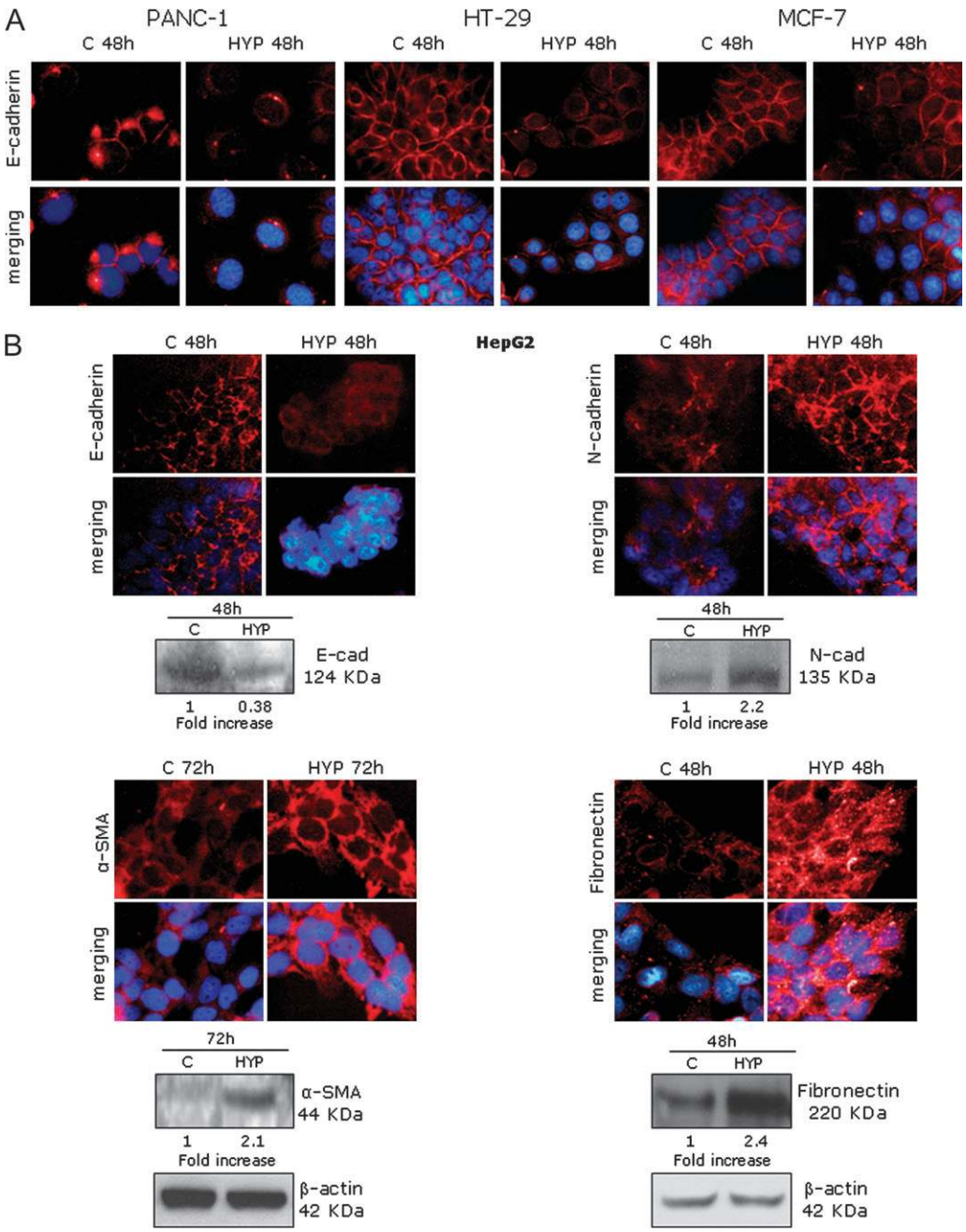

Fig. 1. Hypoxia induces changes in typical markers of EMT. Panel (**A**) expression of E-cadherin in human neoplastic cell lines PANC-1, HT-29 and MCF-7 maintained for 48 h under normoxic conditions (C 48 h) or under hypoxia (HYP 48 h) as shown by indirect immunofluorescence staining. Panel (**B**) expression of E-cadherin, N-cadherin, α-smooth muscle actin (α-SMA) and fibronectin after 48 h incubation under normoxic (C 48 h) or hypoxic conditions (HYP 48 h) in HepG2 cells, chosen as representative model cell line, as shown by indirect immunofluorescence staining and western blot analysis. For immunoblots of α-SMA and fibronectin, sample loading was evaluated by reblotting the same membranes with antibodies raised against β-actin. For immunoblots of E-cadherin and N-cadherin, samples from membrane extracts were evaluated for equal loading by staining in Ponceau S solution (data not shown). For western blot analysis, α-SMA and fibronectin bands were submitted to scanning laser densitometry and then normalized to β-actin; data were then numerically expressed as fold increase versus the respective control bands. In both Panels (A and B) for immunofluorescence analysis, any group of four images is composed by inserts obtained collecting immunopositivity for the selected antigens (top inserts) paralled by the result of their electronic merging with the corresponding images collected for nuclear 4,6-diamidino-2-phenylindole fluorescence (bottom images).

to evaluate chemotaxis (Figure 2C). Of interest, exposure to hypoxic conditions also resulted in an increased release of selected matrix metalloproteinases in the culture medium. Increased release of matrix metalloproteinase-2 was detected in Hep-G2, PANC-1 and MCF-7 cells whereas a significant increased release of matrix metalloproteinase-9 was found only for HepG2 and MCF-7 cells (supplementary Figure 1B is available at *Carcinogenesis* Online).

Mechanisms leading to EMT in cancer cell lines exposed to hypoxia

E-cadherin down-regulation, observed in all cells exposed to hypoxia, is known to play a major role in EMT process; moreover, SNAIL and β-catenin are known to act as major repressors of E-cadherin gene. Along these lines, hypoxia induced nuclear translocation of SNAIL and β-catenin in all human neoplastic cell lines (Figure 3A and B), as observed in both indirect immunofluorescence and western blotting of

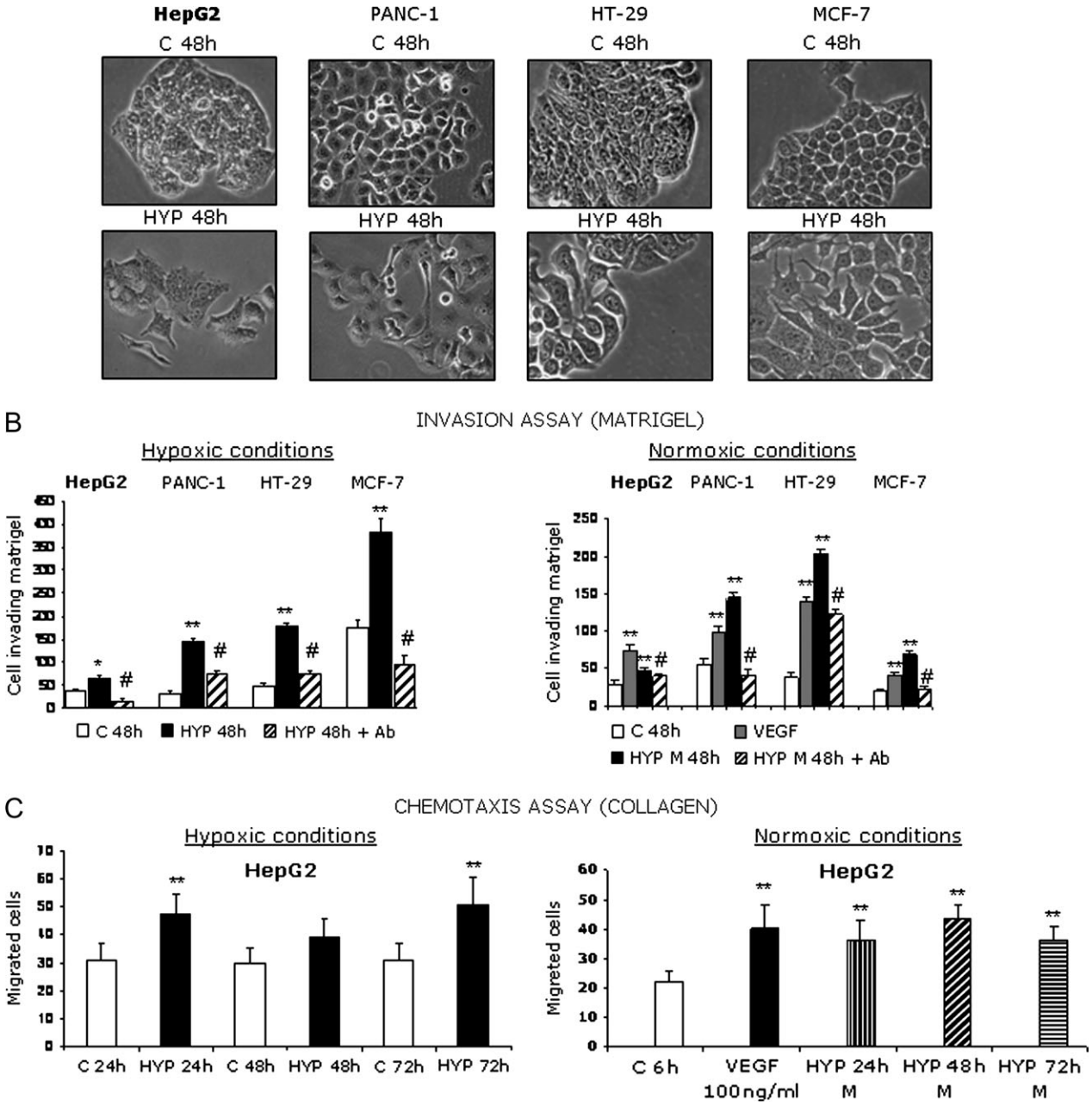

Fig. 2. Hypoxia induces EMT-like fibroblastoid phenotype and increased migration/invasiveness of cancer cells lines. Panel (**A**) phase contrast analysis (original magnification ×100) of morphological changes detected in human neoplastic cell lines in normoxic (C 48 h) or hypoxic (HYP 48 h) conditions. Representative images for all cell lines were collected after 48 h incubation. Panel (**B**) Matrigel invasion assay using Boyden's chambers was performed for all human neoplastic cell lines in hypoxic or normoxic conditions. Hypoxic conditions (left): cells were either not exposed (C 48 h) or exposed to hypoxia (HYP 48 h) for 48 h. When required, cells to be exposed to hypoxic conditions were also pre-treated for 30 min with monoclonal neutralizing antibody raised against Flk-1 (HYP 48 h + Ab). Normoxic conditions (right): cells were either left untreated (C 48 h) or exposed to 100 ng/ml VEGF, used as positive control, or exposed to hypoxic medium collected by cells maintained in hypoxia for 48 h (HYP M 48 h) or, finally, pre-treated for 30 min with monoclonal neutralizing antibody against Flk-1 and then treated with HYP M 48 h (HYP M 48 h + Ab). Panel (**C**) chemotaxis assay using Boyden's chambers was performed only for HepG2 cells, chosen as representative model cell line, in hypoxic or normoxic conditions. Hypoxic conditions (left): cells were either not exposed (C) or exposed to hypoxia (HYP) for the indicated times (24, 48 and 72 h). Normoxic conditions (right): cells were either left untreated (C) or exposed to 100 ng/ml VEGF, used as positive control, or exposed to hypoxic medium collected by cells maintained in hypoxia for 24, 48 or 72 h (HYP M). Data in bar graphs represent mean ± SEM ($n = 4$, in triplicate) of migrated cells. Statistical significance: $^{**}P < 0.001$, $^{*}P < 0.01$ versus control values. $^{\#}P < 0.001$ versus values in cells exposed to hypoxia or hypoxic medium, where appropriate.

nuclear extracts. However, it should be noted that SNAIL translocation was already detectable as soon as 6 h after exposure to hypoxia, whereas nuclear translocation of β-catenin was detected only after 24 (MCF-7 and HT-29 cells) or 48 h of hypoxia (HepG2 and Panc-1 cells).

Nuclear translocation of these two repressors of E-cadherin gene is known to be regulated by the activity of GSK-3β. Exposure of all cell lines to hypoxia induced an early (3 h) phosphorylation and inactivation of GSK-3β (Figure 3C), a result that was inhibited by pre-treating HepG2 cells, chosen as model cell line, with the pharmacological inhibitors of MEK and phosphatidylinositol 3-kinase (PI3-K) PD98095 and LY294002, respectively. These results, potentially suggesting the involvement of multiple signalling pathways in early

GSK-3β phosphorylation and inactivation, were fully confirmed by additional experiments in which the exposure to hypoxic conditions of HepG2 cells resulted in a significant increase of phosphorylation of both Erk1/2 and c-Akt (Figure 3D). Identical results, involving MEK and PI3-K in GSK-3β phosphorylation and inactivation, were also observed for all the other cells used in the study (see supplementary Figure 2A available at *Carcinogenesis* Online).

Since VEGF-A was found to stimulate and sustain invasiveness in all cancer cells (Figure 2B and C), in either normoxic or hypoxic conditions, experiments were designed to investigate the action of the pro-angiogenic cytokine on GSK-3β activity. However, when exposing HepG2 cells under normoxic conditions to human recombinant VEGF-A, no change in GSK-3β phosphorylation status was detected up to 6 h from treatment, suggesting that VEGF was unlikely to trigger early EMT induction (see supplementary Figure 2B available at *Carcinogenesis* Online).

Redox mechanisms contribute to early and hypoxia-dependent GSK-3β phosphorylation and inactivation

In an attempt to identify mechanisms leading to early phosphorylation and inactivation of GSK-3β, a preliminary time course analysis indicated (data not shown) that this event was already detectable as soon as after 15 min of exposure to hypoxic conditions. Accordingly, this early experimental time point was chosen for the following experiments. Inactivation of GSK-3β after 15 min of hypoxia (Figure 4A) was mostly dependent on hypoxia-induced intracellular generation of ROS. Indeed, this early hypoxia-dependent phosphorylation of GSK-3β was prevented by using compounds that are known to inhibit generation of superoxide anion by mitochondria like Rotenone (Rot) or diphenyl-phenylene iodonium (DPI), as shown for HepG2 cells (Figure 4B) as well as for all the other cancer cell lines used (supplementary Figure 2A is available at *Carcinogenesis* Online). Inhibition of GSK-3β phosphorylation was also obtained by pre-treating HepG2 cells with pegylated superoxide dismutase or pegylated catalase before exposure to hypoxia (Figure 4D). Redox sensitivity of GSK-3β was further supported by the fact that low and non-cytotoxic concentrations of hydrogen peroxide (50 μM) were able to reproduce, in normoxic HepG2 cells (Figure 4A and C) as well as in all the other cancer cells (supplementary Figure 2A is available at *Carcinogenesis* Online), early and significant phosphorylation of GSK-3β, reproducing results detected under hypoxic conditions. Along these lines, hydrogen peroxide-dependent phosphorylation of GSK-3β was inhibited by pre-treating HepG2 cells with the pharmacological MEK and PI3-K inhibitors, PD98095 and LY294002, respectively (Figure 4C), once again mimicking data obtained under hypoxic conditions. Moreover, we found that in both hypoxic and normoxic conditions, pre-treatment with okadaic acid, a well-known inhibitor of protein phosphatase 2A, was followed by a very significant increase in GSK-3β phosphorylation (Figure 4A), confirming that GSK-3β phosphorylation was probably to depend on activation of upstream kinases.

In order to have a direct confirmation of intracellular generation of ROS under hypoxic conditions, we used the standard morphological semi-quantitative technique based on the use of 2′,7′-dichlorodihydrofluorescein diacetate. The levels of intracellular fluorescence, due to the interaction of intracellularly generated ROS with the deacetylated dye, were indeed significantly increased in HepG2 cells, chosen as a model cell line, when exposed to hypoxic conditions for 15 min and 3 h or, under normoxic conditions, to 50 μM H_2O_2, the latter used as positive control (Figure 4E). Hypoxia-dependent generation of ROS was abolished by pre-treatment of cancer cells with Rot or DPI. All these data were fully reproduced also in HT-29 cells (Figure 4F), chosen as a model of p53-mutated cell line.

GSK-3β as a key molecule for hypoxia-dependent EMT induction

In order to confirm the major role of GSK-3β in hypoxia-dependent EMT induction, HepG2 cells, cultured under normoxic conditions and chosen as a representative model cell line, were treated either with recombinant human Wnt3A or with lithium chloride (LiCl), a molecule that by inhibiting GSK-3β is known to mimic activation of Wnt/β-catenin-signalling pathway. Both treatments were sufficient to induce EMT-compatible changes, including acquisition of fibroblastoid phenotype (Figure 5A), phosphorylation/inactivation of GSK-3β (Figure 5B), E-cadherin loss of function as well as nuclear translocation of SNAIL and β-catenin (Figure 5C) and a significant increase in chemotaxis and invasiveness (Figure 5D).

Early induction of GSK-3β-dependent EMT-signalling machinery and late increase in invasiveness are distinct events

We next designed experiments in order to unequivocally and mechanistically dissect the role of early generation of ROS from events more likely related to HIF-1α involvement. HepG2 and HT-29 cells (chosen as models of p53 wild-type and p53-mutated cell lines, respectively) were transfected with specifically designed siRNAs against HIF-1α as well as with related non-silencing RNAs. After 72 h, transfected cells, as well as control and non-silencing RNA-treated cells were then exposed to hypoxia for additional 48 h and analysed for HIF-1α levels and invasiveness. Cells transfected with siRNAs against HIF-1α showed a significant down-regulation of HIF-1α levels accounting approximately for a 50–60% decrease versus levels detected in either hypoxic HepG2 or HT-29 cells or in hypoxic cells transfected with non-silencing RNA (Figure 6A and D). Of relevance, both HIF-1α silenced HepG2 and HT-29 cells lost the hypoxia-induced ability to invade Matrigel (Figure 6B and E) that previous experiments disclosed to be mostly dependent on VEGF-A (i.e. a well-known HIF-1α target gene). Indeed, as checked for HepG2 cells, silencing for HIF-1α was effective in significantly decrease VEGF levels released in the culture medium of cells exposed to hypoxia (Figure 6C). Of relevance, early (6 h) hypoxia-induced nuclear translocation of SNAIL was unaffected by silencing of HIF-1α (data not shown) but almost completely abolished by pre-treatment of cells with Rot and DPI (Figure 6F and G), suggesting a dissection between early and ROS-dependent EMT-related changes and late HIF-1α-dependent and VEGF-mediated invasiveness.

Discussion

Hypoxia is a common hallmark of several human malignancies and is currently seen as an independent and unfavourable prognostic factor being associated with a high risk to develop therapy-resistant metastasis (1,3,7–9). Hypoxic conditions within tumour mass have been suggested to favour selection of the most aggressive/invasive neoplastic cells and then, more generally, cancer progression (5,6,10,11).

The present study, performed on different neoplastic cell lines of epithelial origin, suggests the following three major concepts: (i) hypoxia, as an independent factor, is able to switch on an EMT programme leading cancer cells to acquire a fibroblastoid-like phenotype and to display a significantly increased invasive propensity; (ii) hypoxia-induced EMT programme is probably to depend on very early phosphorylation/inactivation of GSK-3β whereas increased invasiveness is significantly sustained by late release of VEGF and (iii) early phosphorylation/inactivation of GSK-3β is significantly regulated by intracellular generation of ROS but unaffected by HIF-1α-dependent mechanisms that are then likely to sustain primarily, through VEGF paracrine–autocrine release, late invasiveness. Although the relevance of EMT in cancer progression has been questioned by some researchers (40), EMT is currently envisaged as one of the steps required by carcinomas to productively expand via invasiveness and intravasation to the surrounding blood vessels (22–25). In our experiments, the simple exposure to hypoxic conditions led cancer cells of epithelial origin to acquire widely accepted features of EMT (22–25), including fibroblastoid phenotype, nuclear translocation of SNAIL, E-cadherin down-regulation, mesenchymal markers (either α-smooth muscle actin or vimentin) and increased migratory/invasive propensity. These data, obtained on cancer cell lines originated from gastrointestinal tumours (HepG2, Panc-1 and HT-29) and breast cancer (MCF-7), confirm and extend previous findings obtained by few other laboratories. A first evidence for a possible relationship between hypoxia,

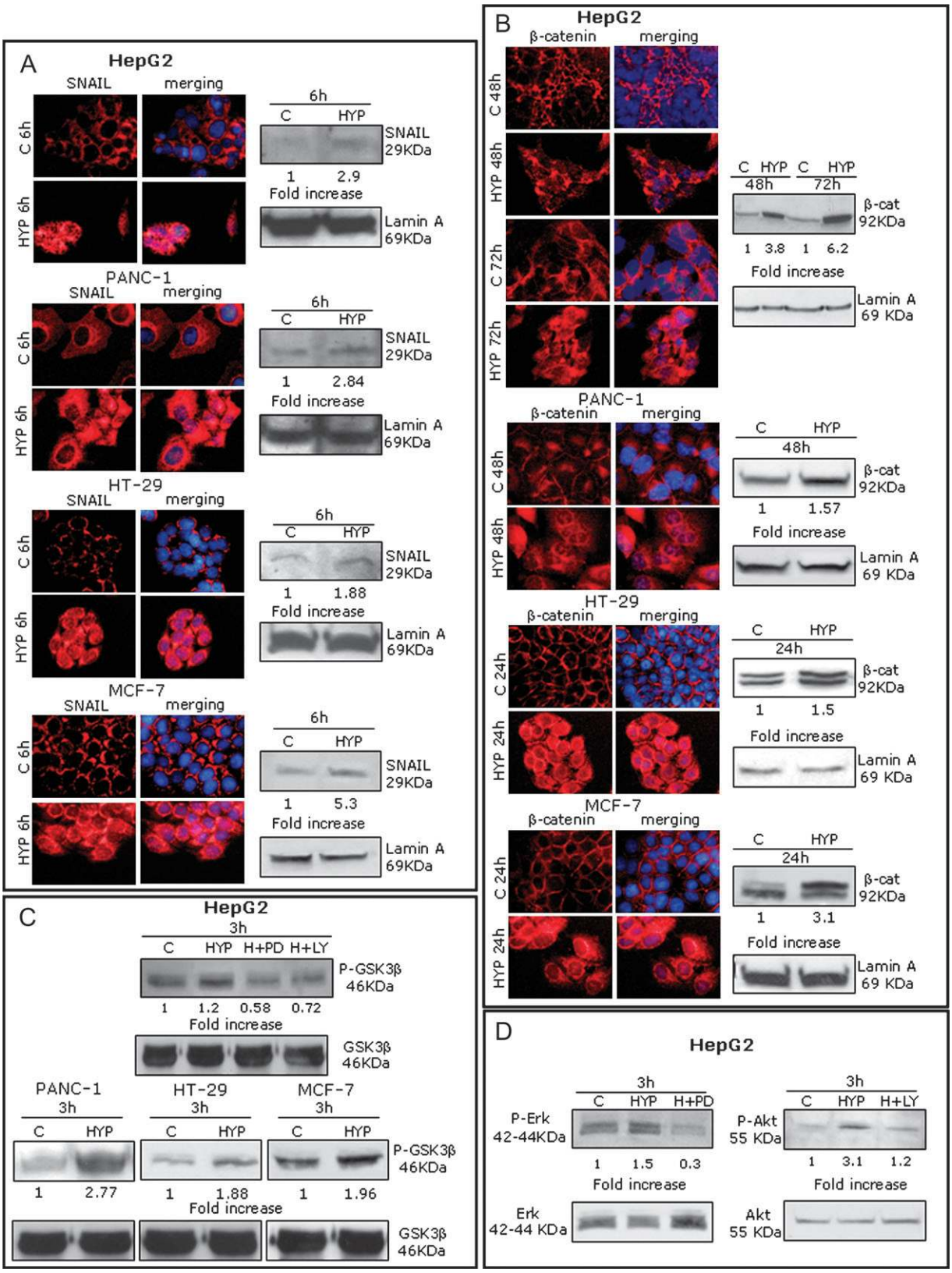

Fig. 3. Hypoxia leads to SNAIL and β-catenin nuclear translocation and involves phosphorylation/inactivation of GSK-3β. Panels (**A** and **B**) cellular localization of SNAIL (A) and β-catenin (B) in the different neoplastic cell lines under normoxic (C) or hypoxic conditions (HYP) as detected by indirect immunofluorescence staining (blue fluorescence, 4,6-diamidino-2-phenylindole staining for nuclei; red fluorescence, SNAIL or β-catenin staining; original magnification ×200) or western blot analysis of nuclear extracts. Experimental time points are indicated. For immunofluorescence analysis, any group of four images is composed by inserts obtained collecting immunopositivity for the selected antigens (left inserts) flanked by the result of their electronic merging with the corresponding images collected for nuclear 4,6-diamidino-2-phenylindole fluorescence (right images). For immunoblots, sample loading was evaluated by reblotting the same membranes with antibodies raised against the nuclear protein Lamin A. Panel (**C**) western blot analysis to detect the state of phosphorylation of GSK-3β in all

SNAIL-related down-regulation of E-cadherin and increased invasiveness was proposed for two ovarian cancer cell lines (41). However, in that study, where EMT was not even mentioned, hypoxia experiments were just designed to complete and support *in vivo* morphological analysis on human ovarian cancers. In a more recent study, Lester *et al.* (42) offered, in our knowledge, the first direct demonstration that hypoxia alone can induce EMT and increased invasiveness using MDA-MB-468 breast cancer cells. In their study, authors obtained results homologous to those provided in the present study (including also GSK-3β phosphorylation and SNAIL translocation). However, they proposed a major mechanistic role for hypoxia-dependent increased expression of the receptor for urokinase-type plasminogen activator (uPAR) and activation of related downstream signalling pathways. This was based on experiments in which silencing or overexpression of uPAR gene was resulting in opposite modulation of EMT. However, in that study, hypoxia-dependent up-regulation of uPAR levels was a relatively late event (i.e. detected at 24 h from the beginning of hypoxia) and EMT was also blocked by antagonizing Rac1 or PI3-K, two putative signalling pathways downstream to uPAR, but not by transfecting cells with a dominant-negative MEK1 construct. This may be of potential relevance taking in mind that the effects of signalling pathways on cell responses are likely to be cell type specific, as shown by the same group using MCF-7 cells in which hypoxia-dependent migration, although at that time seen independently from EMT, was requiring involvement of Ras/Erk pathway (43). Data obtained in the present study suggest an alternative mechanistic interpretation for hypoxia-induced EMT and increased invasiveness. As recalled in the introduction, literature indicates that several signalling pathways can trigger and/or mediate EMT (21–25), including Wnt/β-catenin-signalling machinery. Along these lines, GSK-3β has a widely accepted role in EMT triggering because it is able to control nuclear translocation of both β-catenin and SNAIL (26). These two well-known repressors of E-cadherin gene (22–26) have been also described to act together as a molecular switch for many signalling pathways that lead to EMT (26). In the present study, we show that GSK-3β inactivation is a very early event common to all cell lines employed, being detected within 15 min of hypoxia; moreover, exposure of cancer cells to either recombinant Wnt3A or to LiCl is sufficient to fully reproduce EMT even in normoxic conditions, suggesting a central for GSK-3β inactivation/phosphorylation. These findings prompted us to further investigate mechanisms supporting EMT triggering by hypoxia.

Although hypoxia-dependent HIF-1α overexpression and up-regulation of HIF-1α target genes are common findings in malignant tumours (11–18), our data reasonably exclude HIF-1α-related events in inducing early GSK-3β inactivation/phosphorylation. Along these lines, few studies have analysed the involvement of HIF-1α in EMT (42,44). In a recent study, Yang *et al.* (44) suggested that treatment of L3.6pl pancreatic cancer cells with VEGF-A and VEGF-B resulted in induction of EMT through interaction of these cytokines with VEGF type I receptor (Flt-1). Indeed, in our first set of experiments, we found evidence suggesting that a paracrine–autocrine release of VEGF was relevant for either migration or invasiveness detected under hypoxia. However, when performing more time-dependent and mechanistic experiments, we found that VEGF-A was not able to induce inactivation of GSK-3β up to 6 h and that the use of siRNAs against HIF-1α was unable to prevent early nuclear translocation of SNAIL in HepG2. Conversely, HIF-1α silencing was very effective in abolishing hypoxia-dependent Matrigel invasion of transfected HepG2 and HT-29 cells (chosen as models of p53 wild-type and p53-mutated cancer cell lines, respectively) and then suggesting a possible mechanistic dissociation between early and late events elicited by hypoxia. The very early inactivation (i.e. detected after 15 min) of GSK-3β under hypoxic conditions led us to consider a possible mechanistic role for intracellular generation of ROS, an event that has been extensively described to occur early in cells exposed to low oxygen levels [(45,46) and references therein]. Moreover, massive literature data [(47,48) and references therein] indicate that in either physiological or pathological conditions, intracellular generation of ROS can rapidly trigger and/or modulate several signalling pathways and functional responses in different cells, including signalling pathways related to tumour progression in cancer cells [(48) and references therein]. When analysing this hypothesis, unequivocal evidence for intracellular generation of ROS was detected as early as 15 min after exposure of HepG2 and HT-29 cells to hypoxic conditions, with ROS generation being still significantly increased under hypoxia up to 3 h. Accordingly, early GSK-3β inactivation/phosphorylation was reproduced in all cancer cell lines by simply adding hydrogen peroxide to cells in normoxic conditions or clearly prevented by pre-incubating hypoxic cells with either Rot or DPI which are likely to act in these experimental conditions by inhibiting mitochondrial ROS generation (mitochondria electron transport being the major cellular source responsible for early generation of ROS under hypoxia) (45–48). It should be noted that although DPI is usually also considered as an inhibitor of plasma membrane reduced NADPH-oxidase, here is more likely to act by preventing mitochondrial ROS generation as suggested by the following data: (i) in parallel experiments, we could not prevent early and hypoxia-dependent phosphorylation of GSK-3β by using a more selective reduced NADPH-oxidase inhibitor like apocynin (data not shown); (ii) the effects of Rot and DPI on hypoxia-dependent GSK-3β phosphorylation were, from a quantitative point of view, comparable and (iii) moreover, combined Rot plus DPI pre-treatment failed to afford any additive inhibitory effect on hypoxia-induced GSK-3β phosphorylation.

According to literature, ROS may affect GSK-3β by at least two different signalling mechanisms. Funato *et al.* (49) have recently proposed that ROS may elicit an early, redox-dependent activation of Wnt/β-catenin signalling (but independent on Wnts protein ligands) by affecting the pro-inhibitory, direct interaction between nucleoredoxin (a redox protein belonging to thioredoxin family) and dishevelled resulting in the stabilization of β-catenin and subsequent activation of transcription factor TCF (49). However, in that study, the crucial role for ROS in Wnt/β-catenin signalling was revealed by employing levels of hydrogen peroxide that are definitively higher of those employed in the present study and, more generally, of those believed to be reached within cells (45–48). Accordingly, we could not find any significant involvement of dishevelled in our experimental hypoxic conditions (data not shown). Moreover, as properly discussed by Korswagen [(50) and references therein], one should remind that prolonged exposure to ROS has been reported to even impair Wnt/β-catenin signalling. Interestingly, no study has ascertained whether in cancer cells that have often higher levels of basal intracellular ROS intermediates than normal cells (48), this scenario may apply. In our hypoxic experiments, nuclear translocation of

neoplastic cell lines using specific antibody raised against the phosphorylated form of GSK-3β. Cancer cells of all lines were either not exposed (C) or exposed to hypoxia (HYP) for 3 h. To analyse involvement of Ras/Erk and PI-3K pathways, HepG2 cells were pre-treated with pharmacological inhibitors PD98095 (H + PD) or LY294002 (H + LY), respectively, and then exposed to hypoxia for 3 h. Sample loading was evaluated by reblotting the same membranes with antibody raised against total GSK-3β. Panel (**D**) western blot analysis to detect the state of phosphorylation of Erk 1/2 (p42–p44) or c-Akt in HepG2 cells, chosen as representative model cell line, using specific antibodies raised against the phosphorylated form of Erk1/2 or c-Akt. Sample loading was evaluated by reblotting the same membranes with antibodies raised against the unphosphorylated forms of Erk1/2 or c-Akt. Cells were either not exposed (C) or exposed to hypoxia (HYP) for 3 h. Once again, to analyse involvement of Ras/Erk and PI-3K pathways, HepG2 cells were pre-treated with pharmacological inhibitors PD98095 (H + PD) or LY294002 (H + LY), respectively, and then exposed to hypoxia for 3 h. In all panels, immunodetected bands were submitted to scanning laser densitometry and then normalized to either Lamin A (panels A and B) or total GSK-3β (panel C), Erk or Akt (panel D); data were then numerically expressed as fold increase versus the respective control bands.

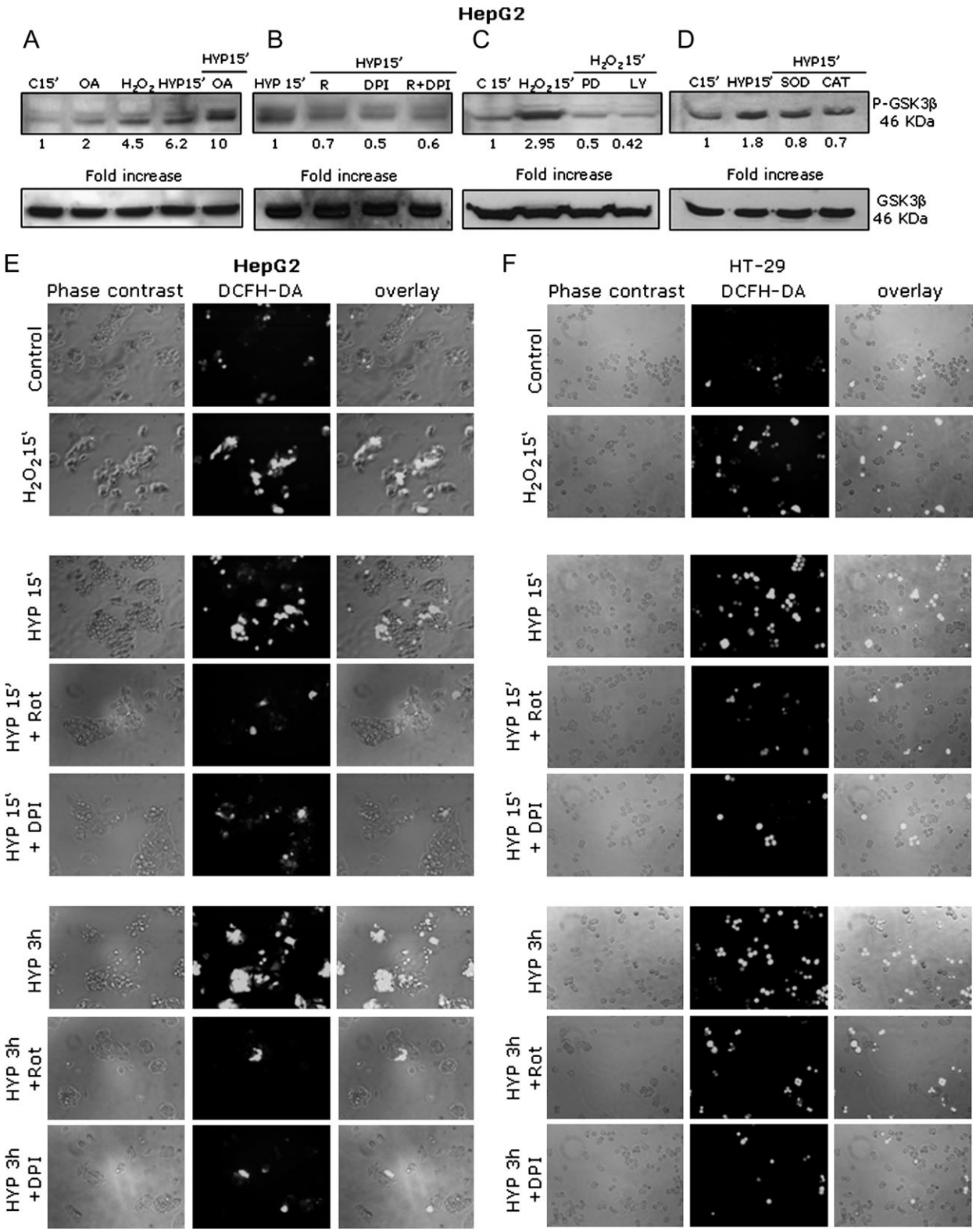

Fig. 4. Intracellular generation of ROS is involved in hypoxia-dependent early phosphorylation/inactivation of GSK-3β. Panels (**A**–**D**) western blot analyses were performed to detect the state of phosphorylation of GSK-3β in HepG2 cells, chosen as representative model cell line, using specific antibody raised against the phosphorylated form of GSK-3β. In order to evaluate the role or ROS, cells were either incubated under normoxic conditions and left untreated (C 15′), treated with 50 μM hydrogen peroxide (H_2O_2), treated with okadaic acid (OA) or exposed to hypoxic conditions (HYP) for 15 min (panel A). In some experiments, before exposure to hypoxic conditions for 15 min, cells were pre-treated for 30 min with a number of molecules including: okadaic acid (HYP 15 min + OA, panel A); the inhibitors of mitochondrial electron transport, Rot (HYP 15 min + R) or DPI as well as Rot in combination with DPI (HYP 15 min + R + DPI) (panel B); pegylated superoxide dismutase or pegylated catalase (HYP15′ SOD and HYP15′ CAT, panel D). Sample loading was evaluated by reblotting the same membranes with antibody raised against total GSK-3β. In order to confirm the putative role of ROS in modulating GSK-3β activity, cells were incubated under normoxic conditions and left untreated (C) or treated with 50 μM hydrogen peroxide (H_2O_2) for 15 min (panel C). In some experiments, before exposure to

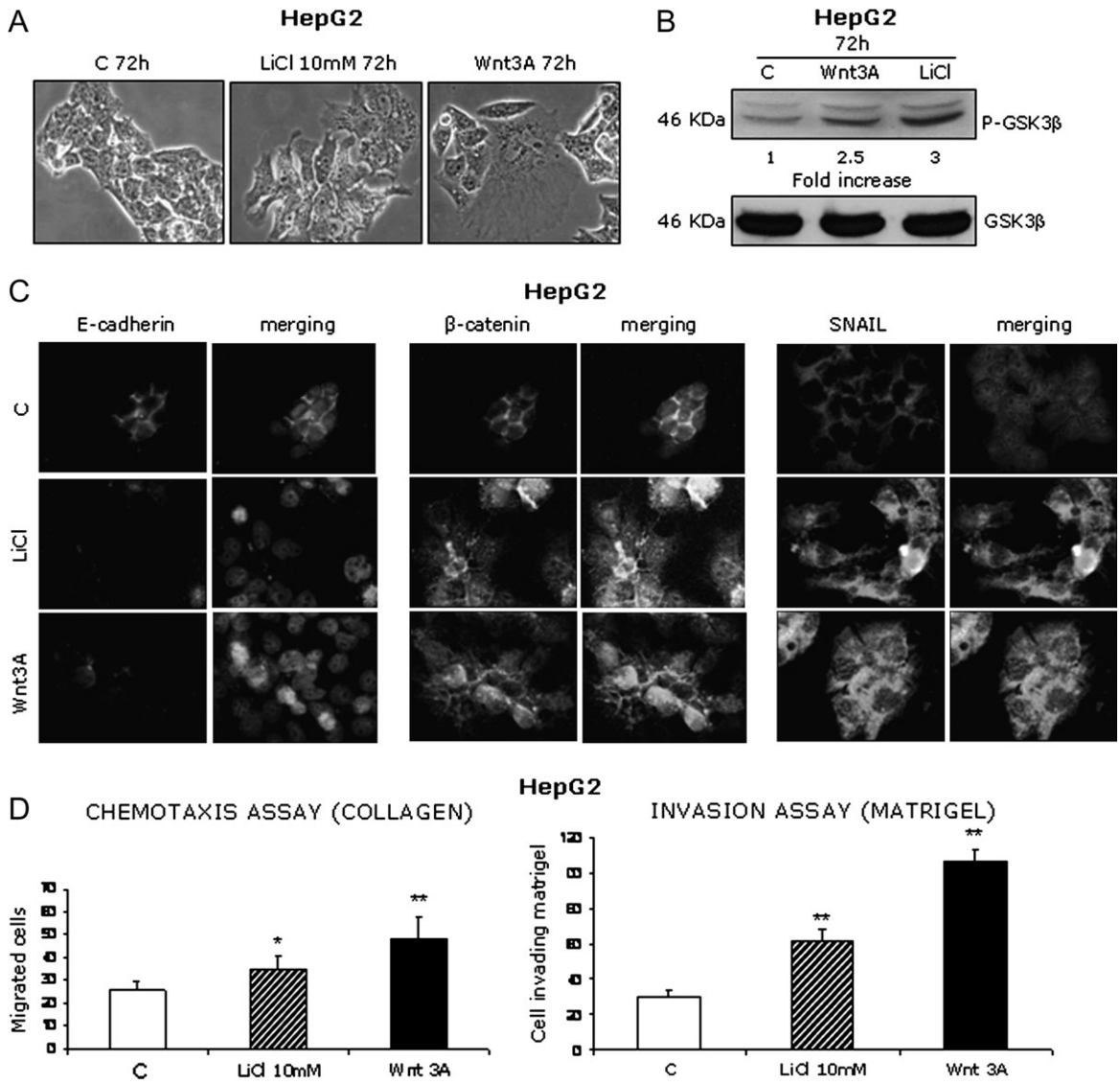

Fig. 5. Phosphorylation/inactivation of GSK-3β is crucial for EMT in cancer cells. Panel (**A**) phase contrast analysis (original magnification ×100) of HepG2 cells, chosen as representative model cell line. HepG2 cells were incubated under normoxic conditions and either left untreated (C) or treated with 10 mM LiCl or with human recombinant Wnt3A for 72 h. Images show evident fibroblastoid-like changes in morphology of cells exposed to LiCl or Wnt3A. Panel (**B**) western blot analysis of GSK-3β phosphorylation in HepG2 cells, chosen as representative model cell line, using specific antibody raised against the phosphorylated form of GSK-3β. Cells were incubated in normoxic conditions and either left untreated (C) or treated with 10 mM LiCl or with Wnt3A for 72 h. Sample loading was evaluated by reblotting the same membranes with antibody raised against total GSK-3β. Immunodetected bands were submitted to scanning laser densitometry and then normalized to total GSK-3β; data were then numerically expressed as fold increase versus the respective control bands. Panel (**C**) expression and cellular localization of E-cadherin, β-catenin and SNAIL in HepG2 cells, shown by indirect immunofluorescence staining (blue fluorescence: 4,6-diamidino-2-phenylindole staining; red fluorescence: E-cadherin or SNAIL staining; green fluorescence: β-catenin staining). Original magnification ×200. HepG2 cells were incubated under normoxic conditions and either left untreated (C) or treated with 10 mM LiCl or with human recombinant Wnt3A for 72 h. For this immunofluorescence analysis, any group of images is composed by inserts obtained collecting immunopositivity for the selected antigens (left insert) flanked by the result of electronic merging with the corresponding images collected for nuclear 4,6-diamidino-2-phenylindole fluorescence (right inserts). Panel (**D**) chemotaxis assay (left graph) and Matrigel invasion (right graph) assays were performed using Boyden's chambers and HepG2 cells. For both assay, cells were incubated in normoxic conditions and either left untreated (C) or treated with 10 mM LiCl or with Wnt3A for 72 h. Data in bar graphs represent mean ± SEM ($n = 4$, in triplicate) of either migrated or invading cells, respectively. Statistical significance: $^{**}P < 0.01$, $^{*}P < 0.05$ versus control values.

hydrogen peroxide for 15 min, cells were pre-treated for 30 min with either the pharmacological inhibitor of Ras/Erk pathway PD98095 (H_2O_2 + PD) or the inhibitor of PI3-K LY294002 (H_2O_2 + LY), respectively (panel C). Sample loading was again evaluated by reblotting the same membranes with antibody raised against total GSK-3β. Representative blots are shown of three independent experiments. In all panels, immunodetected bands were submitted to scanning laser densitometry and then normalized to total GSK-3β; data were then numerically expressed as fold increase versus the respective control bands. Panels (**E** and **F**) detection of intracellular generation of ROS was performed by using the 2′,7′-dichlorodihydrofluorescein diacetate (DCFH-DA) probe in HepG2 cells (panel E) or in HT-29 (panel F), chosen as models of p53 wild-type and p53-mutated cell lines, respectively. Experimental conditions were including the analysis of normoxic cells (Control), normoxic cells treated with H_2O_2 50 μM (H_2O_2) for 15 min (used as positive control) or of cancer cells exposed to hypoxia (HYP) for 15 min and 3 h. In some experiments, before exposure to hypoxic conditions, cells were pre-treated for 30 min with Rot or DPI (HYP 15′ or 3 h + Rot; HYP 15′ or 3 h + DPI). Cells were observed and photographed under a Zeiss fluorescence microscope also equipped with phase contrast objectives. Immunofluorescence and phase contrast images of the same fields were collected and electronically merged (see images in the right column) for all conditions.

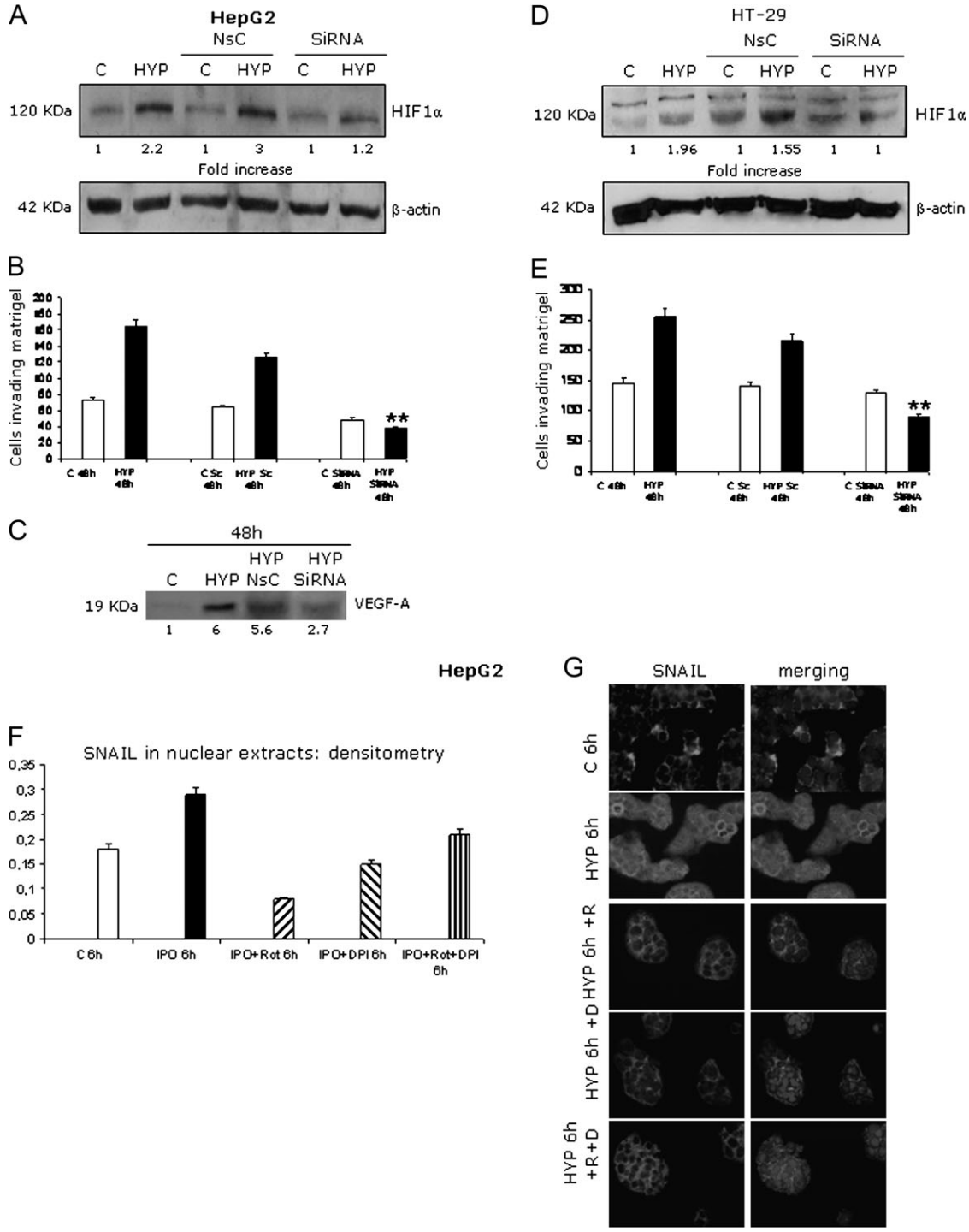

Fig. 6. Dissection of early and late events by experimental manipulations using HIF-1α silencing or inhibition of intracellular generation of ROS. Panels (**A** and **D**) western blot analysis of HIF-1α protein levels was performed either on HepG2 (panel A) and HT-29 cells (panel D) on total extracts obtained from the following experimental conditions: (i) control cells in normoxic conditions for 72 h and then not exposed (C) or exposed for further 48 h to hypoxia (HYP); (ii) cells transfected with non-silencing siRNA up to 72 h and then further exposed for 48 h to normoxic (C–NsC) or hypoxic conditions (HYP–NsC) and (iii) cells transfected with HIF-1α siRNA up to 72 h and then further exposed for 48 h to normoxic (C–siRNA) or hypoxic conditions (HYP–siRNA). Equal loading of samples was monitored on the same blot by detecting β-actin levels. Immunodetected bands were submitted to scanning laser densitometry and then normalized to β-actin; data were then numerically expressed as fold increase versus the respective control bands. Panels (**B** and **E**) the bar graphs show results of the invasion assay that was performed either on HepG2 (panel B) and HT-29 cells (panel E) at the end of 48 h, under normoxic (C) or hypoxic (HYP) conditions, in control cells as well as in cells transfected with either a non-silencing control siRNA (NsC) or a HIF-1α siRNA (siRNA). Panel (**C**) western blot analysis of VEGF protein levels was performed on HepG2 cells, chosen as representative model cell line, by immunoprecipitation technique on culture medium obtained from the following experimental conditions: (i) control cells in normoxic conditions for 72 h and then not exposed (C) or exposed for further 48 h to hypoxia (HYP); (ii) cells transfected with non-silencing siRNA up to 72 h and then further exposed for 48 h to hypoxic conditions (HYP–NsC) and (iii) cells transfected with HIF-1α siRNA up to 72 h and then further exposed for 48 h to hypoxic conditions (HYP–siRNA). Panels (**F** and **G**) expression and cellular localization of SNAIL in normoxic HepG2 cells (C) or in hypoxic HepG2 (HYP 6 h) pre-treated with the inhibitors of mitochondrial electron transfer (complex I), Rot (HYP 6 h + R) or DPI (HYP 6 h + DPI); Rot in combination with DPI (HYP 6 h + R + D). Panel (F) data in the bar graph represent mean ± SEM of densitometric analysis of SNAIL bands

β-catenin was always found as a relatively late event (i.e. significantly detected after at least 24–48 h of hypoxia), a scenario that reasonably excludes ROS as mediators of early and direct activation of Wnt/β-catenin signalling. Hypoxia-dependent early GSK-3β inactivation/phosphorylation seems more compatible with a ROS-dependent early activation of Ras/Erk and PI3-K-signalling pathways, a scenario that has been extensively described in several cell types and under numerous physiological and pathophysiological conditions [(45–48) and references therein]. This interpretation is sustained by the following findings obtained particularly under hypoxic conditions: (i) early induction by hypoxia of increased phosphorylation of Erk1/2 and c-Akt, a feature reproduced also by hydrogen peroxide only in normoxia; (ii) hypoxia-related GSK-3β inactivation/phosphorylation is prevented by pre-incubating cells with either pharmacological inhibitors of MEK1 or PI3-K as well as by employing DPI or Rot and (iii) hypoxia-related GSK-3β inactivation/phosphorylation was strongly increased in either normoxic or hypoxic conditions when cancers cells were pre-treated with okadaic acid, a well-known inhibitor of protein phosphatase 2A. Moreover, the concept of hypoxia-related early generation of intracellular ROS (within the range 15 min to 3 h) as a mechanism leading to persistent GSK-3β inactivation/phosphorylation mediated by ROS-activated Erk1/2 and PI3-K is consistent with the scenario proposed by Zhou *et al.* (26) and fully compatible with early (i.e. 6 h) nuclear translocation of SNAIL that was detected in all cancer cell lines used in this study and was unaffected by HIF-1α silencing.

In conclusion, data reported in the present study [see the schematic diagram in supplementary Figure 3 (available at *Carcinogenesis* Online) that is summarizing the sequence of events] indicate that hypoxia may be seen as an independent factor sufficient to trigger EMT and favour increased invasiveness in a number of cancer cells of epithelial origin. Moreover, although it is likely that other mechanisms (21–26), including those depending on recruitment/stabilization of HIF-1α [perhaps again another feature that has been reported to be favoured by ROS (45)], may consistently contribute to the development of EMT, including invasiveness, we propose that early generation of ROS during hypoxia may represent a 'signal' able to switch on the EMT programme in cancer cells exposed to low levels of oxygen tension.

Supplementary material

Supplementary Figures 1–3 can be found at http://carcin.oxfordjournals.org/

Funding

Regione Piemonte, Torino to M.P.; Fondazione CRT, Torino to M.P.; University of Torino to M.P. and S.C.; Fondazione Bossolasco, Torino to E.N.

Acknowledgements

Conflict of Interest Statement: None declared.

References

1. Vaupel,P. *et al*. (2007) Hypoxia in cancer: significance and impact on clinical outcome. *Cancer Metastasis Rev.*, **26**, 225–239.
2. Harrison,L. *et al*. (2004) Hypoxia and anemia; factors in decreased sensitivity to radiation therapy and chemotherapy? *Oncologist*, **9**, 31–40.
3. Brown,J.M. (1999) The hypoxic cell: a target for selective cancer therapy—eighteenth Bruce F. Cain Memorial Award lecture. *Cancer Res.*, **59**, 5863–5870.
4. Graeber,T.G. *et al*. (1996) Hypoxia-mediated selection of cells with diminished apoptotic potential in solid tumours. *Nature*, **379**, 88–91.
5. Harris,A.L. (2002) Hypoxia—a key regulator factor for tumour growth. *Nat. Rev. Cancer*, **2**, 38–47.
6. Semenza,G.L. (2000) Hypoxia, clonal selection, and the role of HIF-1 in tumour progression. *Crit. Rev. Biochem. Mol. Biol.*, **35**, 71–103.
7. Tatum,J.L. *et al*. (2006) Hypoxia: importance in tumor biology, noninvasive measurement by imaging, and value of its measurement in the management of cancer therapy. *Int. J. Radiat. Biol.*, **82**, 699–757.
8. Höckel,M. *et al*. (1999) Hypoxic cervical cancers with low apoptotic index are highly aggressive. *Cancer Res.*, **59**, 4525–4528.
9. Höckel,M. *et al*. (2001) Tumour hypoxia: definitions and current clinical, biological, and molecular aspects. *J. Natl Cancer Inst.*, **93**, 266–276.
10. Le,Q.T. *et al*. (2004) Hypoxic gene expression and metastasis. *Cancer Metastasis Rev.*, **23**, 293–310.
11. Semenza,G.L. (2002) HIF-1 and tumour progression: pathophysiology and therapeutics. *Trends Mol. Med.*, **8**, S62–S67.
12. Semenza,G.L. (2001) Hypoxia-inducible factor 1: oxygen homeostasis and disease pathophysiology. *Trends Mol. Med.*, **7**, 345–350.
13. Semenza,G.L. (2004) Hydroxylation of HIF-1: oxygen sensing at the molecular level. *Physiology (Bethesda)*, **19**, 176–182.
14. Sharp,F.R. *et al*. (2004) HIF-1 and oxygen sensing in the brain. *Nat. Rev. Neurosci.*, **5**, 437–448.
15. Zhong,H. *et al*. (1999) Overexpression of hypoxia-inducible factor 1 alpha in common human cancers and their metastases. *Cancer Res.*, **59**, 5830–5835.
16. Talks,K.L. *et al*. (2000) The expression and distribution of the hypoxia-inducible factors HIF-1alpha and HIF-2alpha in normal human tissues, cancers, and tumor-associated macrophages. *Am. J. Pathol.*, **157**, 411–421.
17. Semenza,G.L. (2003) Targeting HIF-1 for cancer therapy. *Nat. Rev. Cancer*, **3**, 721–732.
18. Carmeliet,P. *et al*. (1998) Role of HIF-1alpha in hypoxia-mediated apoptosis, cell proliferation and tumour angiogenesis. *Nature*, **394**, 485–490.
19. Thiery,J.P. (2003) Epithelial–mesenchymal transitions in development and pathologies. *Curr. Opin. Cell Biol.*, **15**, 740–746.
20. Bates,R.C. *et al*. (2005) The epithelial–mesenchymal transition (EMT) and colorectal cancer progression. *Cancer Biol. Ther.*, **4**, 365–370.
21. Larue,L. *et al*. (2005) Epithelial–mesenchymal transition in development and cancer: role of phosphatidylinositol 3′ kinase/AKT pathways. *Oncogene*, **24**, 7443–7454.
22. Huber,M.A. *et al*. (2005) Molecular requirements for epithelial–mesenchymal transition during tumour progression. *Curr. Opin. Cell Biol.*, **17**, 548–558.
23. Lee,J.M. *et al*. (2006) The epithelial–mesenchymal transition: new insights in signalling, development, and disease. *J. Cell Biol.*, **172**, 973–981.
24. Thiery,J.P. *et al*. (2006) Complex networks orchestrate epithelial–mesenchymal transitions. *Nat. Rev. Mol. Cell Biol.*, **7**, 131–142.
25. Moustakas,A. *et al*. (2007) Signaling networks guiding epithelial–mesenchymal transition during embryogenesis and cancer progression. *Cancer Sci.*, **98**, 1512–1520.
26. Zhou,B.P. *et al*. (2004) Dual regulation of SNAIL by GSK-3β-mediated phosphorylation in control of epithelial–mesenchymal transition. *Nat. Cell Biol.*, **6**, 931–940.
27. Barallo-Gimeno,A. *et al*. (2005) The Snail genes as inducers of cell movement and survival: implications in development and cancer. *Development*, **132**, 3151–3161.
28. Prindull,G. (2005) Hypothesis: cell plasticity, linking embryonal stem cells to adult stem cell reservoirs and metastatic cancer cells? *Exp. Hematol.*, **33**, 738–746.
29. Aleffi,S. *et al*. (2005) Upregulation of proinflammatory and proangiogenic cytokines by leptin in human hepatic stellate cells. *Hepatology*, **42**, 1339–1348.

(experimental time point: 6 h) in western blots of nuclear extracts. For immunoblots, sample loading was evaluated by reblotting the same membranes with antibodies raised against the nuclear protein Lamin A. Panel (G) indirect immunofluorescence staining to reveal SNAIL immunopositivity in HepG2 cells (blue fluorescence, 4,6-diamidino-2-phenylindole staining; red fluorescence, SNAIL staining). Data and images (panels A, C, D and G) are representative of three different experiments. Data in bar graph of panels (B and E) are expressed as means ± SEM of number of cells invading Matrigel (three experiments for condition) for the indicated conditions. Statistically significant ($^{**}P < 0.01$) versus respective control values.

30. Novo,E. *et al*. (2007) Proangiogenic cytokines as hypoxia-dependent factors stimulating migration of human hepatic stellate cells. *Am. J. Pathol.*, **170**, 1942–1953.
31. Willert,K. *et al*. (2003) Wnt proteins are lipid-modified and can act as stem cell growth factors. *Nature*, **22**, 448–452.
32. Parola,M. *et al*. (1998) HNE interacts directly with JNK isoforms in human hepatic stellate cells. *J. Clin. Invest.*, **102**, 1942–1950.
33. Robino,G. *et al*. (2000) Interaction between 4-hydroxy-2,3 alkenals and the platelet-derived growth factor-beta receptor. Reduced tyrosine phosphorylation and downstream signalling in hepatic stellate cells. *J. Biol. Chem.*, **275**, 40561–40567.
34. Zamara,E. *et al*. (2004) 4-Hydroxynonenal as a selective profibrogenic stimulus for activated human hepatic stellate cells. *J. Hepatol.*, **40**, 60–68.
35. Novo,E. *et al*. (2006) Overexpression of Bcl-2 by activated human hepatic stellate cells: resistance to apoptosis as a mechanism of progressive hepatic fibrogenesis in humans. *Gut*, **55**, 1174–1182.
36. Romanelli,R.G. *et al*. (2006) Thrombopoietin stimulates migration and activates multiple signaling pathways in hepatoblastoma cells. *Am. J. Physiol. Gastrointest. Liver Physiol.*, **290**, G120–G128.
37. Rezvani,H.R. *et al*. (2007) Hypoxia inducible factor 1α, a key factor in the keratinocyte response to UVB exposure. *J. Biol. Chem.*, **282**, 16413–16422.
38. Novo,E. *et al*. (2006) Dose dependent and divergent effects of superoxide anion on cell death, proliferation and migration of human hepatic stellate cells. *Gut*, **55**, 90–97.
39. Autelli,R. *et al*. (2005) Intracellular free iron and acidic pathways mediate TNF-induced death of rat hepatoma cells. *Apoptosis*, **10**, 777–786.
40. Tarin,D. *et al*. (2005) The fallacy of epithelial mesenchymal transition in neoplasia. *Cancer Res.*, **65**, 5996–6000.
41. Imai,T. *et al*. (2003) Hypoxia attenuates the expression of E-cadherin via up-regulation of SNAIL in ovarian carcinoma cells. *Am. J. Pathol.*, **163**, 1437–1447.
42. Lester,R.D. *et al*. (2007) uPAR induces epithelial mesenchymal transition in hypoxic breast cancer cells. *J. Cell Biol.*, **178**, 425–436.
43. Lester,R.D. *et al*. (2005) Erythropoietin promotes MCF-7 breast cancer cell migration by an ERK/mitogen-activated protein kinase-dependent pathway and is primarily responsible for the increase in migration observed in hypoxia. *J. Biol. Chem.*, **280**, 39273–39277.
44. Yang,A.D. *et al*. (2006) Vascular endothelial growth factor receptor 1 activation mediates epithelial to mesenchymal transition in human pancreatic carcinoma cells. *Cancer Res.*, **66**, 46–51.
45. Kietzmann,T. *et al*. (2005) Reactive oxygen species in the control of hypoxia-inducible factor-mediated gene expression. *Semin. Cell Dev. Biol.*, **16**, 474–486.
46. Guzy,R.D. *et al*. (2005) Mitochondrial complex III is required for hypoxia-induced ROS production and cellular oxygen sensing. *Cell Metab.*, **1**, 401–408.
47. Dröge,W. (2002) Free radicals in the physiological control of cell function. *Physiol. Rev.*, **82**, 47–95.
48. Wu,W.-S. (2006) The signalling mechanisms of ROS in tumour progression. *Cancer Metastasis Rev.*, **25**, 695–705.
49. Funato,Y. *et al*. (2006) The thioredoxin-related redox regulating protein nucleoredoxin inhibits Wnt-β-catenin signalling through dishevelled. *Nat. Cell Biol.*, **8**, 501–508.
50. Korswagen,H.C. (2006) Regulation of the Wnt/β-catenin pathways by redox signalling. *Dev. Cell*, **10**, 687–688.

Received May 30, 2008; revised September 1, 2008;
accepted September 6, 2008